Probing vacancies in NiO nanoparticles by EXAFS and molecular dynamics simulations

A Anspoks, A Kalinko, R Kalendarev and A Kuzmin

Institute of Solid State Physics, University of Latvia, Riga, LV-1063, Latvia

E-mail: andris.anspoks@cfi.lu.lv

Abstract. In this work we apply a combination of classical molecular dynamics (MD) and *ab initio* multiple-scattering EXAFS approach (MD-EXAFS methodology) to study the influence of point defects (Ni vacancies) on the structure and lattice dynamics of NiO nanoparticles. A NiO nanoparticles model, able to reproduce the experimental Ni K-edge EXAFS spectra, has been developed and allowed us to obtain original information on the particle size, the amount of Ni vacancies, thermal disorder and atomic structure relaxation.

1. Introduction

Nanosized nickel oxide (NiO) shows an increase of the lattice parameter upon decreasing of the particle size, as is evidenced by x-ray diffraction [1]. EXAFS spectroscopy reveals a decrease of the first shell Ni–O_1 average distance by ∼0.02-0.04 Å and an increase of the mean second shell Ni–Ni_2 distance by ∼0.01-0.02 Å for pure $Ni_{1-x}O$ and vanadium doped $Ni_{1-x}V_xO_y$ thin films [2, 3]. At the same time, an elongation of the first shell Ni–O_1 and the second shell Ni–Ni_2 distances has been found in ultra fine NiO particles dispersed on activated carbon fibers [4]. Such structure relaxation is closely connected with the nanoparticles size and surface as well as the presence of defects in the bulk. Recently, the presence and the role of the Ni vacancies have been studied by EXAFS in sputtered NiO films [5, 6] and nanoparticles [7] based on the analysis of the first two shells. It has been proposed that the distribution of the Ni vacancies in NiO nanoparticles, having a size of 10–18 nm, can be considered within a core-shell model [7].

In this work we evaluate the effects of the NiO nanoparticles size and the presence of Ni vacancies employing a recently developed simulation method [8], based on the use of classical molecular dynamics with *ab initio* multiple-scattering EXAFS calculations (MD-EXAFS methodology). Such approach allowed us to go beyond the limitations of the conventional EXAFS analysis procedure.

2. Experimental and data analysis

Two different NiO nanocrystalline samples, nanoparticles (nano-NiO) and thin film (tf-NiO), were studied in comparison with commercial microcrystalline NiO (c-NiO, Aldrich, 99%), having green color. Black color of nano-NiO and dark brown color of tf-NiO indicate the presence of the Ni vacancies [9]. Sample preparation details were reported previously in [10, 11]. According to the Scherrer's method and assuming the cubic crystallites shape, the average size of nanocrystallites was around 6 nm. The Ni K-edge x-ray absorption spectra were measured in

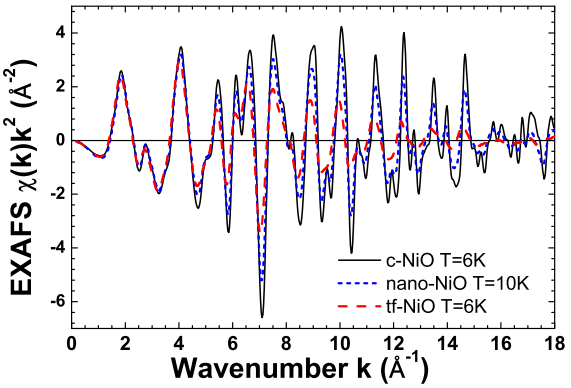

Figure 1. Low temperature Ni K-edge EXAFS spectra $\chi(k)k^2$ for polycrystalline NiO, NiO nanoparticles and thin film.

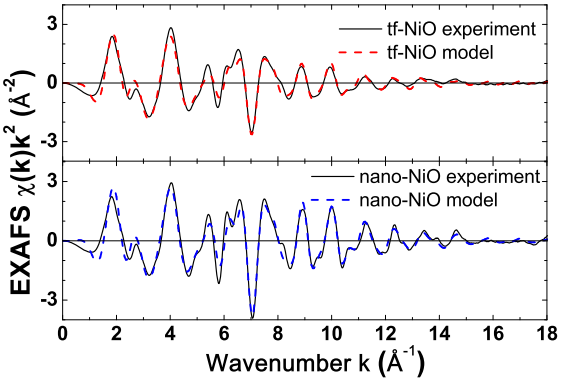

Figure 2. Comparison of the experimental and configuration-averaged Ni K-edge EXAFS spectra $\chi(k)k^2$ for nano-NiO and tf-NiO at T=300 K.

transmission mode at the HASYLAB/DESY C1 bending-magnet beamline in the temperature range from 6 K to 300 K. Details of experiments can be found in [10, 11].

The EXAFS oscillations $\chi(k)$ were extracted and analysed following the conventional procedure [12] using the EDA software package [13]. Noticeable difference between the EXAFS spectra of microcrystalline and nanocrystalline samples is clearly visible due to the static disorder caused by the atomic structure relaxation near the nanocrystallite surface and around defects (Fig. 1). The contribution from the first two coordination shells was analysed in the single-scattering approximation [11]. The values of the interatomic distances for the 1st (Ni–O_1, ±0.002 Å) and 2nd (Ni–Ni_2, ±0.003 Å) coordination shells of Ni at low temperature are, respectively, 2.088 Å and 2.952 Å for c-NiO, 2.082 Å and 2.961 Å for nano-NiO, 2.084 Å and 2.969 Å for tf-NiO. This result is in agreement with previous EXAFS works [2, 3].

3. MD-EXAFS simulations

The scheme of our MD-EXAFS calculations is shown in Fig. 3. First, we selected the cubic model for the nanoparticles with the size $L \times L \times L$. It was generated starting from the unit cell containing 4 Ni and 4 O atoms and having the lattice parameter a_0=4.173 Å as for c-NiO [1]. The required concentration of Ni vacancies (C_{vac}) was introduced by removing randomly selected Ni atoms in order to achieve uniform distribution of the vacancies in the particle.

Our force-field (FF) potential model includes two-body central force interactions between atoms and is described by a sum of the Buckingham and Coulomb potentials with the values reported in [11, 14]. The charge of nickel atoms Z_{Ni} was selected as the optimization parameter, and the charge of the oxygen atoms Z_{O} was calculated to fulfill electroneutrality condition. In our model all Ni ions have the same charge and so do all oxygen ions. All other Buckingham potential parameters have been left unchanged as for c-NiO [11, 14].

MD simulations were performed using the DLPOLY4.02 code [15], which is suitable for both crystalline and nanosized materials with huge number of the particles. Crystalline c-NiO was modeled in the isothermal-isobaric NPT ensemble using the supercell $6a_0 \times 6a_0 \times 6a_0$ and 3D periodic boundary conditions. The nanosized NiO particles were simulated in the canonical NVT ensemble with the nanoparticle placed in the middle of a large empty box. All simulations were performed at 300 K and zero pressure corresponding to the conditions of the EXAFS experiment. Technical details of calculations have been reported previously in [10, 11].

For each nanoparticle with the given size L and Ni vacancy concentration C_{vac} we performed

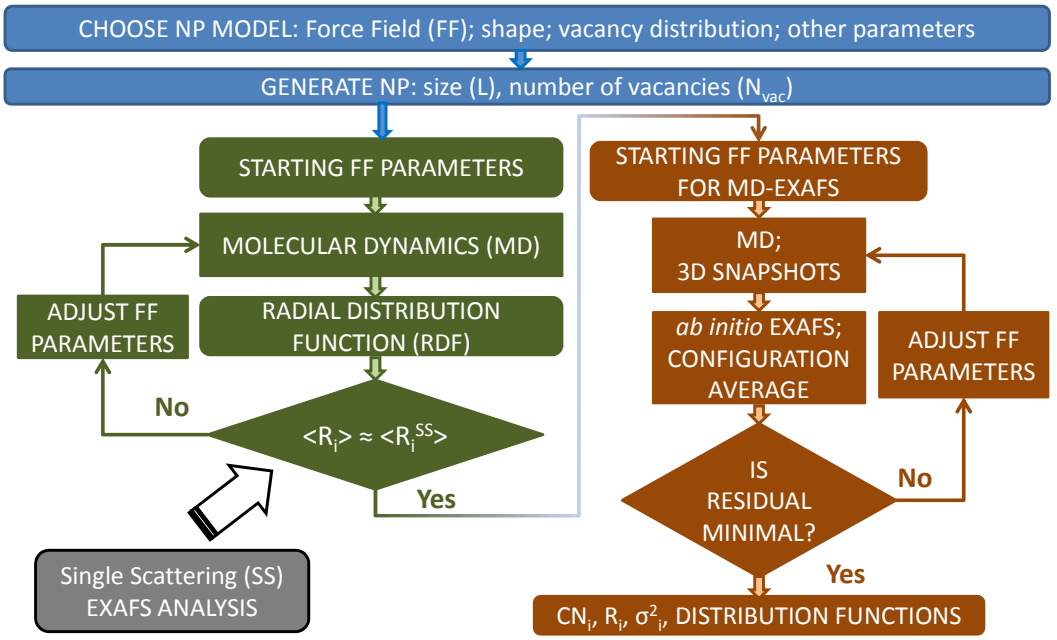

Figure 3. Scheme of the MD-EXAFS calculations for nanoparticles (NP).

MD calculations with two different FF parameter values (in our case two different Z_{Ni} values: +2.0 and +1.9). Then we found the corresponding interatomic distance $R(\mathrm{Ni–Ni_2})$ and compared it with the value obtained from the conventional EXAFS analysis using the single-scattering approximation $R^{SS}(\mathrm{Ni–Ni_2})$. If two values do not coincide within the desired precision, then we adjust FF parameters for the next iteration. This process is repeated until the required precision is achieved. At the end, we found for each nanoparticle with the size L and the vacancy concentration C_{vac} the FF parameters, which give the same value of the average $\mathrm{Ni–Ni_2}$ distance as the one obtained from conventional EXAFS analysis.

At the next step (see the right part of the scheme in Fig. 3), the residual between the experimental and configuration-averaged (CA) EXAFS spectra for the model nanoparticle is used as a criterion for the FF model optimization and to evaluate the quality of the nanoparticle model. At each iteration step, we calculate a set of atomic configuration snapshots using classical MD. The number of snapshots depends on the nanoparticle material, size and shape as well as on the experimental conditions, i.e. pressure and temperature, and should ensure the convergence of the CA EXAFS spectrum. We found that EXAFS spectra from at least 4000 absorbers are required to achieve convergence. For EXAFS calculations we used *ab initio* real-space multiple-scattering FEFF8 code [16], and the technical details of calculations were reported in [10, 11].

Further we will describe the algorithm of the FF optimization. We start from the results of the previous step and calculate the CA EXAFS spectra for two MD simulations, obtained using slightly different (usually ±0.005) Z_{Ni} values. Then we compare residuals between the experimental and CA EXAFS spectra and guess new value of Z_{Ni} in order to minimize the residual value. Here we change Z_{Ni} value in steps within the desired precision (in our case ±0.005). When the residual minimum is reached, we stop the MD-EXAFS calculations and evaluate all other required properties from the MD data, for example, values of coordination numbers CN_i, interatomic distances R_i, and MSRDs σ_i^2 for each i coordination shell.

As the first application of the described procedure we optimized the ions charges for c-NiO. The best fit to its EXAFS spectrum was achieved with Z_{Ni}=+2.015 and Z_{O}=–2.015.

Next we have studied the reliability of our FF model in a description of the local atomic structure relaxation around the Ni vacancy in the bulk of c-NiO. Our results show that the six nearest oxygen atoms move away from the center of the vacancy by ≈0.2 Å, thus significantly shortening the distances to nearest Ni atoms. At the same time, twelve nearest Ni atoms move slightly towards the center of the vacancy by ≈0.08 Å, thus increasing the distance with their neighbouring Ni atoms. Such relaxation of atomic structure, induced by the presence of single Ni vacancy, plays significant role in the average structure relaxation, especially for the first coordination shell of Ni, as was found recently [5]. The results of our simulations are in excellent agreement with those from the recent *ab initio* calculations [17, 18], which predict the relaxation of O atoms by about 0.17 Å outwards from the Ni vacancy site. This result confirms that our simple FF potential model reproduces well structure relaxation around the Ni vacancies.

Finally we have simulated NiO nanoparticles, starting from the initially cubic shape. The size of the cube L and the concentration of the nickel vacancies $C_{\rm vac}$ were chosen as model parameters, which were optimized by minimizing the residual between the experimental and CA Ni K-edge EXAFS spectra (Fig. 2). A well defined residual minimum has been found indicating the reliability of the model. The best agreement was achieved for nanoparticles with non-zero concentration of the Ni vacancies: $C_{\rm vac}$≈0.4-1.2% for NiO nanoparticles with the size of L≈3.6-4.2 nm and $C_{\rm vac}$≈1.6-2.0% for NiO thin film with the size of L≈1.3-2.1 nm.

4. Conclusions

We report on the recently developed complex simulation approach, combining classical MD and *ab initio* multiple-scattering EXAFS theory, which allows us to reliably simulate both bulk and nanosized materials using small number of adjustable model parameters (L, $C_{\rm vac}$, Z). The method leads to better use of the rich information hiding in the EXAFS spectra, which is particulary interesting for nanosized objects. The application of the method to nickel oxide allowed us to evaluate the size of nanoparticles and the concentration of nickel vacancies.

Acknowledgments

The authors are grateful to Dr. R. Chernikov for assistance during EXAFS measurements at DESY. This work was supported by ESF Project 2009/0202/1DP/1.1.1.2.0/09/APIA/VIAA/141 and Latvian Government Research Grant No. 09.1518. The EXAFS experiments at HASYLAB/DESY have been supported from the European Community's Seventh Framework Programme under grant agreement No. 226716 (Project I-20100110 EC).

References

[1] Li L, Chen L, Qihe R and Lia G 2006 *Appl. Phys. Lett.* **89** 134102
[2] Kuzmin A, Purans J and Rodionov A 1997 *J. Phys.: Condens. Matter* **9** 6979
[3] Avendaño E, Kuzmin A, Purans J, Azens A, Niklasson G A and Granqvist C G 2005 *Phys. Scripta* **T115** 464
[4] Hattori Y, Konishi T and Kaneko K 2002 *Chem. Phys. Lett.* **355** 37
[5] Jang W L, Lu Y M, Hwang W S, Hsiung T L and Wang H P 2009 *Appl. Phys. Lett.* **94** 062103
[6] Jang W L, Lu Y M, Hwang W S, Dong C L, Hsieh P H, Chen C L, Chan T S and Lee J F 2011 *Europhys. Lett.* **96** 37009
[7] Mandal S, Banerjee S and Menon S R 2009 *Phys. Rev.* B **80** 214420
[8] Kuzmin A and Evarestov R A 2009 *J. Phys.: Condens. Matter* **21** 055401
[9] Sato H, Minami T, Takata S and Yamada T 1993 *Thin Solid Films* **236** 27
[10] Anspoks A, Kuzmin A, Kalinko A and Timoshenko J 2010 *Solid State Commun.* **150** 2270
[11] Anspoks A and Kuzmin A 2011 *J. Non-Cryst. Solids* **357** 2604
[12] Aksenov V L, Kuzmin A Yu, Purans J and Tyutyunnikov S I 2001 *Phys. Part. Nucl.* **32** 675
[13] Kuzmin A 1995 *Physica* B **208-209** 175
[14] Fisher C A J 2004 *Scr. Mater.* **50** 1045
[15] Todorov I T, Smith W, Trachenko K and Dove M T 2006 *J. Mater. Chem.* **16** 1611
[16] Ankudinov A L, Ravel B, Rehr J J and Conradson S D 1998 *Phys. Rev.* B **58** 7565
[17] Ferrari A M and Pisani C 2007 *J. Chem. Phys.* **127** 174711
[18] Park S, Ahn H S, Lee C K, Kim H, Jin H, Lee H S, Seo S, Yu J and Han S 2008 *Phys. Rev.* B **77** 134103